Disentangling the effect of heritability and plasticity on *Populus fremontii* leaf reflectance across a temperature gradient

Seeley, M. M.[1*†]; Thomson, E.[2*]; Allan, G. J[3]; Whitham, T. G. [3]; Hultine, K. R.[4]; Cooper, H. F.[3,5]; Wiebe, B. C.[6]; Asner, G. P.[1]; Jaclyn P. M. Corbin[3,6]; Doughty, C.E.[6]

1. Center for Global Discovery and Conservation Science, Arizona State University, Hilo, HI 96706
2. School of Geography & the Environment, University of Oxford, Oxford, UK
3. Department of Biological Sciences and Center for Adaptable Western Landscapes, Northern Arizona University, Flagstaff, AZ 86011, USA
4. Department of Research, Conservation and Collections, Desert Botanical Garden, 1201 North Galvin Parkway, Phoenix, AZ 85008, USA
5. Center for Adaptable Western Landscapes, Northern Arizona University, Flagstaff, AZ 86011, USA
6. School of Informatics, Computing, and Cyber Systems, Northern Arizona University, Flagstaff, AZ, USA

*Equal first authors

†Corresponding author; mseeley1@asu.edu

ORCID iDs

Megan M. Seeley https://orcid.org/0000-0003-1945-1162

Eleanor Thomson https://orcid.org/0000-0003-1670-8970

Gerard J. Allan https://orcid.org/0000-0002-8007-4784

Thomas G. Whitham https://orcid.org/0000-0002-1262-4342

Kevin Hultine https://orcid.org/0000-0001-9747-6037

Hillary F. Cooper https://orcid.org/0000-0003-2634-1404

Benjamin C. Wiebe https://orcid.org/0000-0002-9325-1540

Gregory P. Asner https://orcid.org/0000-0001-7893-6421
Jaclyn P. M. Corbin https://orcid.org/0000-0001-6769-4471
Christopher E. Doughty https://orcid.org/0000-0003-3985-7960

Keywords
Populus fremontii, cottonwood, spectroscopy, hyperspectral, plasticity, heritability, genotypic variation, extreme temperatures; forest; tree; heat

Summary

- We quantified the relative effect of plasticity and heritability on *Populus fremontii* (Fremont cottonwood) leaf reflectance using clonal replicates propagated from 16 populations and grown across three common gardens spanning a mean annual temperature gradient of 10.7–22.3°C.
- We used variance partitioning to decompose phenotypic variation expressed in the leaf spectra into genotypic versus environmental components and estimate broad-sense heritability and found that heritability was most strongly expressed in the red-edge (~680-750nm) and SWIR (~1400-3000nm).
- Support vector machine models predicted *P. fremontii* source population and garden location at 78% and 93% accuracy, respectively, demonstrating that genotypic and environmental variation can be differentiated from the same leaf spectra. However, model accuracy declined by ~49% when using leaf reflectance from any two common gardens to predict the source population at the third site. Prediction accuracies were lowest for the hottest site, which was linked to leaf stress responses in the visible and red-edge wavelengths (400-750nm).
- We conclude that leaf spectra display heritability and plasticity across different parts of the spectrum. When mapping in regions/seasons with extreme climates, spectral plasticity linked to heat stress can decrease spectral heritability but may offer opportunities to understand phenological responses to extreme temperatures at large scales.

Introduction

Globally, forests are threatened by climate change as increasing temperatures and drought have led to widespread tree mortalities (Allen et al., 2010). Many regions have already experienced declines in biodiversity, and these declines are predicted to accelerate (O'Neill et al., 2017; Pachauri et al., 2014; Pimm et al., 2014; Rull and Vegas-Vilarrúbia, 2006; Thomas et al., 2004). Remote sensing, specifically imaging spectroscopy, has emerged as a conservation tool that can inform and improve decision-making at the landscape scale (Rose et al., 2015; Seeley & Asner, 2021; Turner et al., 2003). For example, forest conservation applications of imaging spectroscopy include accurate, high-resolution species mapping (Asner et al., 2008; Balzotti et al., 2020; Pengra et al., 2007; Seeley, Vaughn, Shanks, et al., 2023; Skowronek et al., 2017; Somers & Asner, 2013; Torabzadeh et al., 2019), large-scale biodiversity estimations to inform and support protected area establishment (Asner et al., 2017; Féret and Asner, 2014), and monitoring forest health (Asner et al., 2016; Brodrick and Asner, 2017; Roberts et al., 2003; Vaughn et al., 2018; Weingarten et al., 2021). Heritable, intraspecific trait variation is required for species to be able to keep pace with a changing climate and adapt to novel climate conditions. However, phenotypic variation in leaf spectra can arise from both genotypic and environmental variations in nutrient abundance, herbivore and pathogen pressure, or climate conditions. Disentangling genotypic versus environmental sources of spectral variation is vital for developing remote sensing methods that can distinguish both standing genotypic variation within a species and explore how climate change is affecting leaf traits and overall plant function.

Spectroscopy is a remote sensing tool that captures a continuous portion of the electromagnetic spectrum, allowing for the estimation of leaf traits (Asner et al., 2015; Asner and Martin, 2016, 2009; Munaiz et al., 2020; Townsend et al., 2003; Ustin and Gamon, 2010; Wang et al., 2020), plant health (Brodrick & Asner, 2017; Christen et al., 2007; Cotrozzi, 2022; Degerickx et al., 2018; Seeley, Martin, Giardina, et al., 2023; Shendryk et al., 2016; Weingarten et al., 2021), and variation in genotypic expression (Asner & Martin, 2009; Blonder et al., 2020; Cavender-Bares et al., 2016; Čepl et al., 2018; Czyż et al., 2020; Madritch et al., 2014; McManus et al., 2016; Schweiger et al., 2018; Seeley, Stacy, Martin, & Asner, 2023). While many leaf traits and indicators of plant health are directly expressed in spectra, non-parametric models have typically been used to relate leaf spectra to phylogenetic information, based on the assumption that species, genotypes, and other genetically related individuals display a unique 'fingerprint' of

heritable traits. Yet few studies have attempted to quantify the link between leaf spectra and heritability across the whole VSWIR spectra, as plant clones, or known genetic relationships, are required to separate heritability from the environmental response. A notable exception is Čepl et al. (2018) who quantified the narrow-sense heritability of *Pinus sylvestris* spectra, using genetic information reconstructed from DNA markers.

Heritability is a statistic used in the field of genetics that estimates the degree of variation in a phenotypic trait that is due to genetic variation between individuals of a population. Measuring heritability in plant traits has long been a practice in selective breeding programs searching for heritable traits to maximize yield and quality (Bradshaw, 2017). Broad-sense heritability is defined as $H^2=v(G)/v(E)$, where v(G) is the proportion of genetic variance and v(E) is the proportion of environmental variation, typically quantified using clonal replicates (Hühn, 1975). Thus, broad-sense heritability can vary according to the amount of environmental variation experienced by individuals. As spectroscopy integrates a vast array of leaf traits in its analyses and has been shown to be a better predictor of plant and ecosystem function than a subset of foliar traits (Madritch et al., 2014; Yan et al., 2021), quantifying heritability across a reflectance spectrum may yield novel insights into genetic versus environmental controls on leaf spectra, linked to functional traits, and reveal parts of the spectrum useful for retrieving phylogenetic information.

In this study, we used a common garden experiment to understand plastic and genotypically constrained responses of leaf reflectance spectra in *Populus fremontii* (Fremont cottonwood). While plasticity has a genetic component (Cooper et al., 2019; Laitinen and Nikoloski, 2019; Scheiner, 1993), we simplified our discussion of plasticity here as the degree to which leaf spectra change across different environments. *Populus fremontii* inhabits riparian zones in the southwestern United States and Mexico and is recognized as one of the most important foundation species in these regions (Ellison et al., 2005; Whitham et al., 2006) due to its ability to structure communities across multiple trophic levels, drive ecosystem processes, and influence biodiversity via genotypically based functional trait variation (Ferrier et al., 2012; Grady et al., 2013). As a foundation species, *P. fremontii* is often used in riparian restoration projects (Grady, 2012; Nagler et al., 2007). Despite active planting projects, the areal extent of *P. fremontii* has declined dramatically over the last century due to water extraction, competition with invasive species, and climate change (Braatne et al., 1996; Glenn et al., 1998; Shafroth et

al., 1995; J. Stromberg, 1998; Stromberg, 2001) and its six ecotypes are projected to differentially shift their geographical distributions (Bothwell et al., 2023; Ikeda et al., 2017). Consequently, *P. fremontii* gallery forests are considered among the most threatened forest types in North America. To support management decisions for *P. fremontii* and protect riparian ecosystems vulnerable to climate change, it is necessary to improve large-scale mapping of *P. fremontii* response and tolerance to changing climate conditions and quantify the heritable resilience, or the intraspecific variation in plant traits that could result in greater ecosystem resilience (Turner, 2023; Vahsen et al., 2023), of *P. fremontii* populations to drought and extreme temperatures.

To determine the influence of heritability and plasticity on reflectance spectra, we collected handheld leaf reflectance spectra from *P. fremontii* clonal replicates propagated from 16 populations across the American Southwest and grown at three common garden sites. The gardens span the full thermal range of *P. fremontii* from the hottest site, Yuma, on the Arizona/Mexican border where the mean warmest month temperature exceeds 33.8°C, to the coldest site in Canyonlands, Utah, where the mean coldest month temperature drops to -3.2°C. We determined the source of variation (environmental versus genotypic) across the spectra to determine which regions demonstrated the highest heritability and which parts exhibited higher spectral plasticity across the different common garden sites, with spectral plasticity being the variation in reflectance spectra attributed to the common garden site. As Yuma experiences extreme temperatures where ambient temperatures could exceed the critical temperature at which Photosystem II is disrupted (t_{crit}) (Moran et al., 2023), we were able to assess the response of leaf spectra when trees experienced air temperatures approaching and surpassing their critical leaf temperature thresholds (Hultine et al., 2020; Moran et al., 2023). Through this, we aimed to 1) determine whether intraspecific spectral variation was driven primarily by the common garden site or source population, 2) assess the effect of extreme temperature on leaf-level reflectance spectra, 3) identify which regions of the VSWIR spectra were conserved and which regions varied across the common gardens, and 4) determine the potential of large-scale classifications of heritable *P. fremontii* intraspecific variation.

Materials and Methods

Study Sites

Three common garden sites were established across the thermal range of *P. fremontii* in 2014. Two were located at the thermal edges of the *P. fremontii* temperature range (Yuma, Arizona: 22.8°C and Canyonlands, Utah: 10.7°C), and one garden was in the middle of this range (Agua Fria, Arizona: 17.2°C; Figure 1; Table 1). A detailed description of the common garden establishment can be found in Cooper et al. (2019, 2022). Each garden hosted cuttings from sixteen geographically separate (minimum 13.5 km) *P. fremontii* populations across Arizona spanning 12.2ºC Mean Annual Temperature. From each cutting, clonal replicates were propagated in a greenhouse. 32 clonal replicates of each cutting were planted in each common garden, across 4 stratified random blocks to minimize the effect of within-garden variation on a population. In total, each common garden hosted 16 wild populations of *P. fremontii*, eight genotypes (cuttings) from each population, and 32 clonal replicates from each genotype, resulting in 4096 *P. fremontii* saplings per garden.

Three of the cottonwood source populations were located on the Mogollon Rim in the Colorado Plateau and are part of the Utah High Plateau/Mogollon Rim ecotype (Blasini et al., 2021; Ikeda et al., 2017). The remaining thirteen populations represented the environmental range of the Sonoran Desert. Within the Sonoran Desert ecotype, two ecotypes (northern and southern) were identified (Bothwell et al., 2023). The larger of the clades in the northern Sonoran Desert includes nine source populations and is referred to as the main Sonoran Desert cluster, while the southeast (SE) Sonoran Desert cluster includes three populations in the southeastern portion of Arizona. Lastly, one population (KWF) did not fall into either Sonoran Desert cluster. Trees at the common gardens were routinely watered to facilitate establishment in the arid southwest.

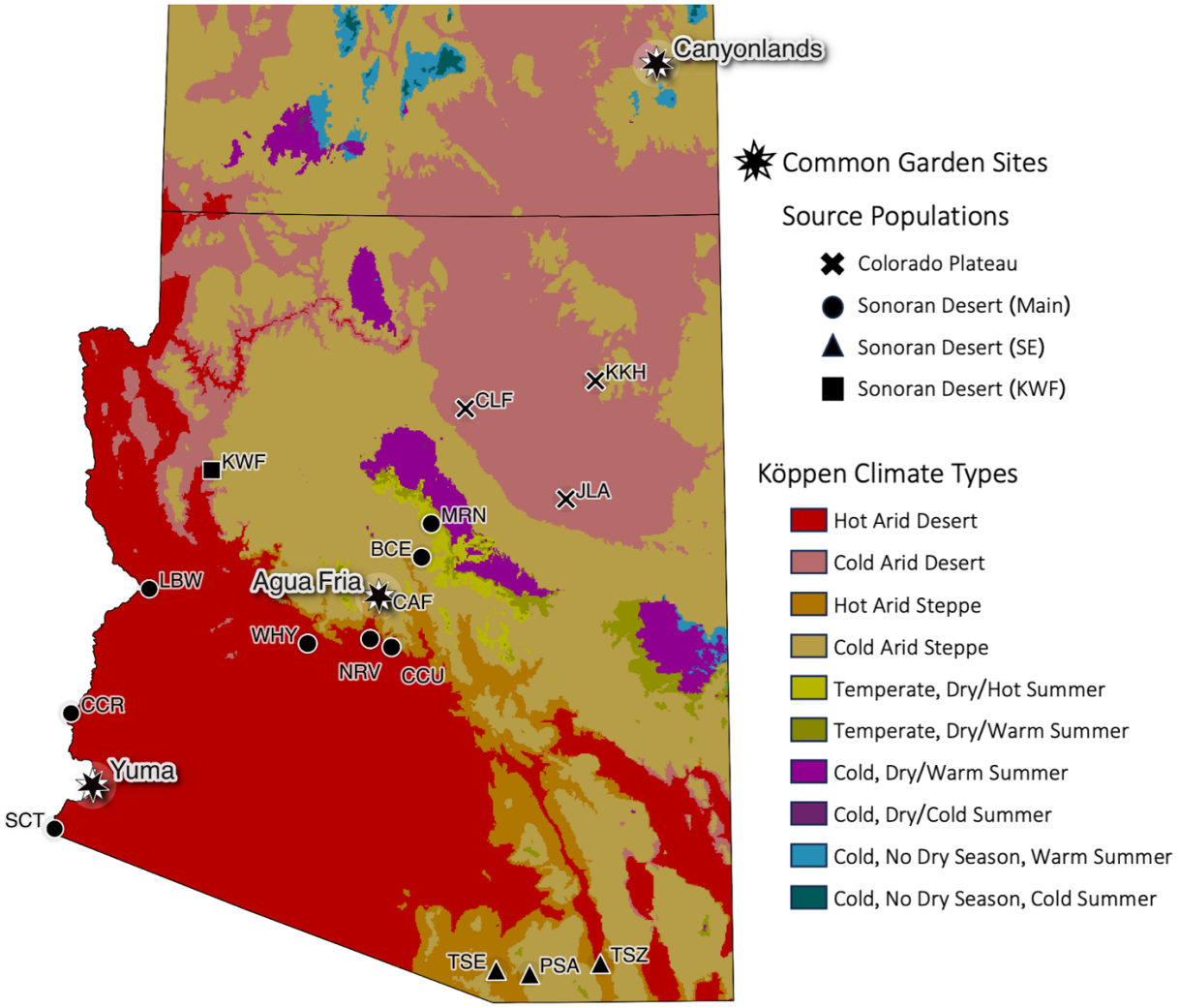

Figure 1: Source population and common garden site locations in Arizona and southern Utah. Background colors represent Köppen climate types.

Source Population	Elevation	Mean Annual Temperature (°C)	Mean Annual Precipitation (mm)	Ecotype
MRN	1774	10.4	593	Sonoran Desert Main
KKH	1920	10.7	258	Colorado Plateau
JLA	1507	12.3	212	Colorado Plateau
CLF	1299	14.1	176	Colorado Plateau
KWF	1126	15	243	Sonoran Desert KWF
BCE	1109	15.6	432	Sonoran Desert Main

PSA	1234	15.7	471	Sonoran Desert SE
TSZ	1219	16.9	322	Sonoran Desert SE
CAF	988	17.2	440	Sonoran Desert Main
TSE	986	17.5	402	Sonoran Desert SE
WHY	575	19.6	284	Sonoran Desert Main
CCU	696	19.9	349	Sonoran Desert Main
NRV	666	19.9	337	Sonoran Desert Main
SCT	26	22.1	88	Sonoran Desert Main
LBW	143	22.3	137	Sonoran Desert Main
CCR	70	22.6	97	Sonoran Desert Main
Common Garden Site				
Canyonlands	1581	10.7	225	
Agua Fria	998	17.2	453	
Yuma	49	22.8	93	

Table 1: Source population and study site environmental conditions. For source populations, the ecotype is listed.

Leaf Measurements

We measured leaf reflectance spectra from trees at the three common gardens in May 2018, four years after the saplings had been planted. Due to the differential survivorship of the saplings, the number of trees sampled from each population at each garden varied (0-52; Table S1). For each tree, three leaves were collected. Where possible, leaves were harvested from different branches. Only full-expanded, sunlit adult leaves were chosen. Leaves were harvested by hand and transported in a cool box to the nearby field station for processing the same day.

Spectral measurements were collected using a leaf clip and Analytical Spectra Devices (ASD) field spectrometer from 350 to 2500 nm at 1-nm intervals (Analytical Spectra Devices Inc., Boulder, CO, USA). Measurements were taken on the adaxial surface of the leaf in the center. Three spectral readings were taken per leaf, and each measurement consisted of 25 internally averaged reflectance readings. The spectrometer was optimized using a white reference taken after every three leaves. To minimize noise, wavelengths with a low signal-to-noise ratio were removed; this included reflectance values below 400 nm and above 2450 nm.

Next, brightness normalization was applied to all spectral measurements to minimize variation not related to leaf chemistry and structure (Kruse et al., 1993; Myneni et al., 1989). Leaf spectra from the same individual were then averaged.

Leaf trait measurements and analyses

Following spectral measurements, leaves were scanned using a digital scanner (Canon LiDE 110) to determine their area, oven dried at 70 ◦C for three days and weighed for their dry mass. Leaf mass per area (LMA) was calculated by dividing the leaf's dry mass (g) by its fresh one-sided area (m^2).

The degree of stress experienced by each tree was estimated by calculating the photochemical reflectance index (PRI) (Equation 1; Thénot et al., 2002).

Equation 1:

$$PRI = \frac{\rho_{531} - \rho_{570}}{\rho_{531} + \rho_{570}}$$

PRI quantifies the normalized difference between ρ_{531}, the reflectance at 531 nm, and ρ_{570}, that at 570 nm, to capture xanthophyll pigment content and epoxidation state in leaves. The quantity and epoxidation state of xanthophyll pigments in leaves respond to plant stress and are an indicator of thermal tolerance and photosynthetic efficiency (Gamon et al., 1992). PRI has been used as an indicator of plant stress at both the leaf and airborne levels (Buddenbaum et al., 2015; Hernández-Clemente et al., 2011; Kohzuma et al., 2021; Rossini et al., 2013; Suárez et al., 2010).

To determine whether the common garden sites induced changed in leaf traits across the same populations, a Tukey-Kramer multiple comparison test was applied to the LMA data. The Tukey-Kramer test from the scipy python package allowed us to perform a pairwise comparison between the different sites and does not require equal sample sizes (Virtanen et al., 2020). LMA was further plotted via boxplots according to the common garden site and source population. Differences in PRI for each source population across the common garden sites were similarly compared using boxplot diagrams and the Tukey-Kramer test.

Phenotypic variation in leaf spectra

To explore spectral variation in the three common gardens, we plotted the mean source population spectra at each common garden site. Source population spectra were colored according to garden location. As there were visual differences in mean spectra based on site in the visible range (400-700 nm), we compared peak values in the visible range across common gardens using the same Tukey-Kramer multiple comparison test above.

Spectral differences between the same populations at different common garden sites were further visualized using principal component analysis (PCA). PCA reduces the dimensionality of the spectral data from over 2000 dimensions to a handful of dimensions that explain the primary spectral variation across multiple channels (Boardman and Green, 2000; Green and Boardman, 2000; Thompson et al., 2017). As PCA requires equal sample sizes to reduce bias, five populations were used (CLF, KWF, BCE, PSA, and SCT), as these populations had the largest number of samples (104) and were represented in all three common gardens. Using scikit-learn (Pedregosa et al., 2011), PCA was applied to the five populations and the first two principal components (PC) were plotted along the x and y axes. While the first two PC have the greatest explained variance for the dataset, higher PC are often important in spectroscopy applications for discriminating differences in surface chemistry and other traits (Dai et al., 2022; Seeley, Martin, Vaughn, et al., 2023; Thompson et al., 2017).

To visualize the spectral differences between populations in the higher dimensional PCs, the distances between ecotype centroids in the first 20 PC were calculated and plotted according to the methods described in Seeley, Martin, Vaughn, et al. (2023). The same five source populations were used across Agua Fria and Canyonlands and grouped according to ecotype. Ecotypes included the Colorado Plateau, Sonoran Desert Main, and Sonoran Desert Southeast (SE). Spectral data from Yuma was excluded from this analysis, as Yuma created a significant shift in reflectance spectra linked to heat stress (Figure 3). Standardizing the source populations and their sample sizes allowed us to compare the effects of environmental variation on the same ecotypes present in different gardens and the effects of genotypic variation on different ecotypes present in the same garden.

Decomposing genotypic and environmental variation across the spectra and estimating broad-sense heritability

To quantify the relative effects of environmental versus genotypic variation across the visible to shortwave infrared (VSWIR) spectrum, we used variance partitioning to decompose observed variance at each wavelength into the relative contribution of site, ecotype, population, genotype, or clone. All sampled data was used across all common garden sites. Following the method of Asner et al. (2014) and Fyllas et al. (2009), variance partitioning was calculated using a linear mixed-effects model for each wavelength across the VSWIR spectra using the lme4 *R* package (Bates et al., 2015). The model was fitted using Residual Maximum Likelihood (REML). All effects were treated as random. Common garden site was included as a crossed random effect, while clones were nested within genotypes, which were nested within populations, which were nested within ecotype. The total spectral variance about the mean for a given wavelength was, therefore, quantitatively parsed into the variance explained by site ($\sigma 2_s$), cottonwood ecotype ($\sigma 2_e$), populations within ecotype ($\sigma 2_p$), genotypes within populations ($\sigma 2_g$), clones within genotypes ($\sigma 2_c$) and residual variance ($\sigma 2_r$):

$$\sigma 2_{total} = \sigma 2_s + \sigma 2_e + \sigma 2_p + \sigma 2_g + \sigma 2_c + \sigma 2_r$$

Using the results of the linear mixed-effects model, we next calculated broad-sense heritability across the spectrum. Heritability at each wavelength was calculated using the classic broad sense heritability equation ($H^2 = V_G/V_P$), where V_G is genotypic variation, and V_P is total variation ($V_G + V_E$). Variance explained by ecotypes, populations, and genotypes is categorized as genotypic variance (V_G), as the genetic material within these groups differs. Variance explained by site and clones, as well as residual variance, is categorized as environmental variation (V_E), or spectral plasticity, as the genetic material within these groups is identical, so any observed differences in the spectra must be due to environment or measurement error. Broad-sense heritability was plotted across the VSWIR spectrum. This analysis was applied first to data from all three sites and then to data from Canyonlands and Agua Fria alone. To obtain confidence intervals for H^2, we employed a nonparametric bootstrap approach. Bootstrapping, a method commonly used for obtaining uncertainty estimates for heritability (Schweiger et al., 2016; Thai et al., 2013), involves resampling the dataset with replacement and recalculating the variance with each subsampled dataset. We performed 1000 iterations for each wavelength, sampling 31 spectra from each common garden x ecotype combination, resulting in n=279 for

each iteration. The mean variation and H^2 of the 1000 iterations were presented along with the 95% confidence interval calculated from the bootstrapped H^2 estimates.

Using leaf spectra to predict genotypic and environmental information

To explore whether the leaf spectra could be used to extract both genotypic and environmental information, we used a support vector machine (SVM) and leaf spectra across the three sites to predict *P. fremontii* source population (genotypic variation), ecotype (genotypic variation) and garden location (environmental variation). SVMs efficiently handle highly dimensional datasets by creating decision boundaries in n-dimensional space that maximize the distance between class boundaries and sample points (Melgani and Bruzzone, 2004). SVMs tend to outperform other machine learning algorithms such as random forest for species and genotype classifications when applied to spectroscopy data (Baldeck et al., 2014; Balzotti & Asner, 2018; Dalponte et al., 2012; Feret & Asner, 2013; Melgani & Bruzzone, 2004; Sampaio et al., 2020; Seeley, Vaughn, & Asner, 2023; Seeley, Vaughn, Shanks, et al., 2023; Xie et al., 2009). For each radial basis function kernel SVM, we optimized hyperparameter selection through a cross-validation grid search implemented in python with the scikit-learn package (Pedregosa et al., 2011).

As SVMs can be biased when class sizes are unequal, the same five source populations were used as above (CLF, KWF, BCE, PSA, and SCT). To maintain consistent class sizes, 104 samples from each garden were randomly selected. For the ecotype prediction, only data from Agua Fria and Canyonlands were included to facilitate comparison with the PCA analysis above. To maintain consistent class sizes, 47 samples from each ecotype at Canyonlands and Agua Fria were randomly selected. For all models – source population, common garden site, and ecotype – data were divided into training/test datasets using a 70/30 stratified random split. Test data were used to calculate accuracy and develop confusion matrices for each model.

To assess the universality of the models in predicting genotypic information in unseen and extreme environments, we further trained the *P. fremontii* source population model on spectra from two of the gardens and tested it on unseen spectra from the third garden. A different garden was withheld each time, resulting in three models. This allowed us to compare the applicability of the model in extreme environments and assess how well the model can extrapolate outside of its training data.

Results

Leaf trait results

Among the sites, LMA differed at $p = 0.05$ according to the Tukey-Kramer test (Figure 2b). LMA increased along the temperature gradient with increasing air temperature. LMA was lowest at Canyonlands, with a mean LMA of 72.9 g/m^2 and a standard deviation of 10.2 g/m^2 across all populations. LMA averaged 88.1 g/m^2 at Agua Fria with a standard deviation of 19.1 g/m^2, while Yuma exhibited the highest LMA at 108.4 g/m^2 with a standard deviation of 11.2 g/m^2. Agua Fria demonstrated the most variation in LMA while both Canyonlands and Yuma were more constricted in their LMA range. While the mean LMA at Agua Fria was closer to that at Canyonlands, the maximum LMA at Agua Fria was only two g/m^2 less than that at Yuma (146.7 and 148.7 g/m^2, respectively).

Mean PRI, the plant stress indicator where more negative values indicate greater plant stress, was 0.018 for both Agua Fria and Canyonlands but decreased to -0.011 for Yuma. According to the Tukey-Kramer test, Yuma was the only common garden site that differed in PRI from the other gardens. PRI did not vary significantly based on the source population.

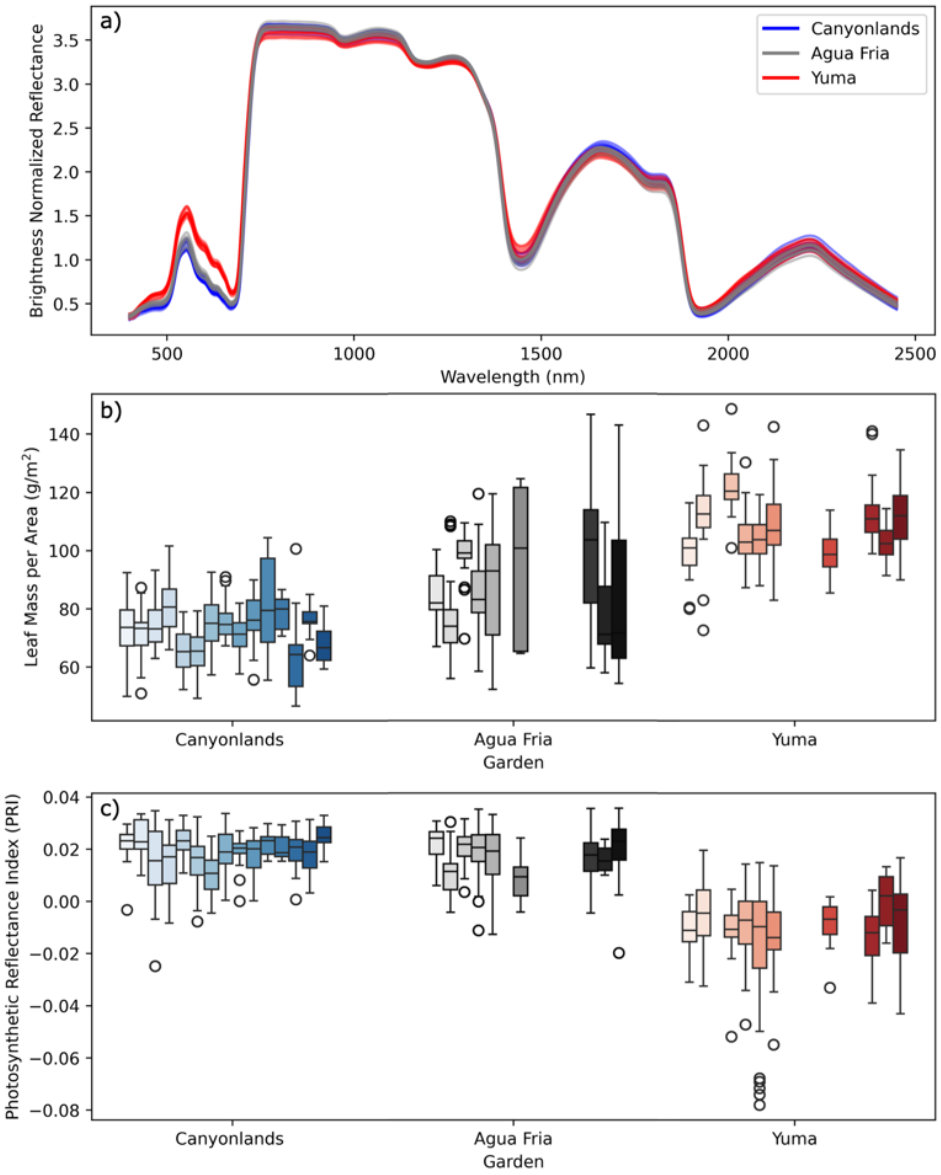

Figure 2: a) Mean brightness normalized reflectance of each source population at each of the three common garden sites. See Figure S1 for reflectance prior to brightness normalization. b) Boxplots of *Populus* leaf mass per area (LMA) and c) photosynthetic reflectance index (PRI) categorized by source population and site. Within each garden, boxplots are ordered according to source population mean annual temperature, with cooler populations on the left and warmer populations on the right. Gaps correspond to populations that were not sampled at a given garden. Note that boxplots represent a different number of sampled trees per population per site.

Leaf spectral results

Leaf spectral analysis revealed diverging leaf characteristics among the gardens, especially at Yuma. Mean brightness normalized reflectance plotted according to population and site demonstrated a separation in the visible range between Yuma and the other sites (Figure 2a; see Figure S1 for reflectance prior to brightness normalization). The mean peak in the visible range (400 nm – 700 nm) was 1.17 (unitless) for Canyonlands, 1.21 for Agua Fria, and 1.54 for Yuma. According to the Tukey-Kramer multiple comparison test, the maximum peak (551-556 nm) of spectra in the visible range from the three common garden sites was different at p=0.05.

Spectral differences between the sites were further explored using PCA (Figure 3). The first two principal components of the reflectance spectra explained 57.8 and 35.3% of the variance, respectively (Figure 3a). Together, these axes separated Yuma spectra from Canyonlands and Agua Fria, as the five populations sampled from Yuma (CLF, KWF, BCE, PSA, and SCT) clustered away from the same five populations sampled at the other sites.

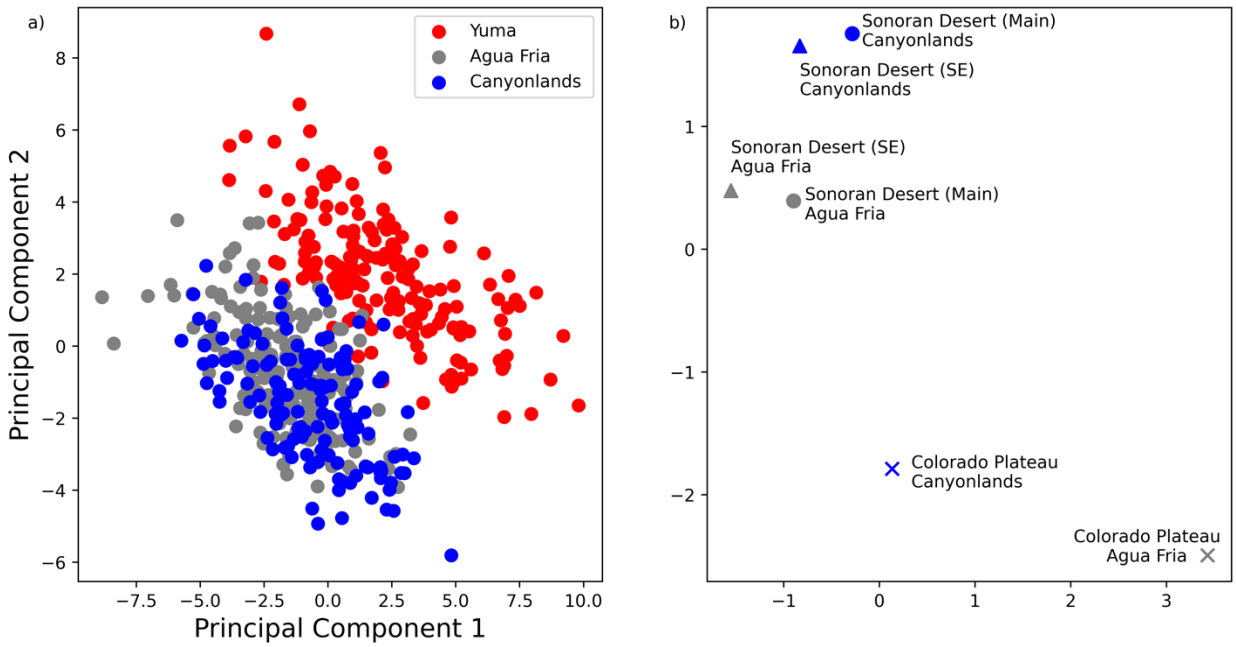

Figure 3: a) First and second principal components of leaf spectra colored according to the common garden site. b) Distance between the centroids of source population grouped by ecotype x common garden plotted in principal component space. Shapes correspond to the ecotype (x: Colorado Plateau, circle: Sonoran Desert Main, triangle: Sonoran Desert SE), and colors represent the common garden (blue: Canyonlands, grey: Agua Fria).

Variance partitioning and broad-sense heritability analysis

Across all gardens, spectral variance was highest in the visible (~500-670 nm) and red-edge wavelengths (~680-750 nm). When Yuma was included in the analysis, variance in these wavelengths was driven largely by the common garden site (as demonstrated in Figures 2 and 3) and heritability in these regions was correspondingly low with a maximum heritability of 0.08 and 0.43 for the visible and red-edge, respectively (Figure 4). While heritability peaks near the red edge were present regardless of the inclusion of Yuma in the analysis, the peak was shifted toward longer wavelengths when Yuma was excluded. When Yuma was excluded from the analysis, site-level variation in the visible (~500-670 nm) and red-edge wavelengths (~680-750 nm) was minimal. Instead, variance at these wavelengths was driven more by genetic factors (population and genotype), with corresponding high spectral heritability (~0.36 and ~0.66, respectively).

Across all gardens, reflectance heritability in the *P. fremontii* trees was greatest in the short-wave infrared region (SWIR; 1400 – 2450 nm) followed by the transition from red-edge to near-infrared (NIR; ~750 nm), regardless of the inclusion of Yuma (Figure 4). In the shorter wavelengths of the NIR (~750-1140 nm) and SWIR, site-level variation explained less of the variance than genotypic factors in general, and the spectral differences caused by Yuma were relatively minimal, resulting in high heritability (max: 0.51 min: 0.31). When Yuma was excluded, heritability peaked in the red-edge (740 nm; heritability: 0.67). The NIR had a negative relationship with wavelength length until ~1320 nm where heritability increased and remained high in the SWIR, although it varied across this region (max: ~0.56, min: ~0.37). Across the VSWIR, particularly heritable regions of the spectra included the red-edge/NIR transition (~750 nm) and the SWIR. More environmentally sensitive (plastic) regions included the visible and red-edge as well as much of the NIR.

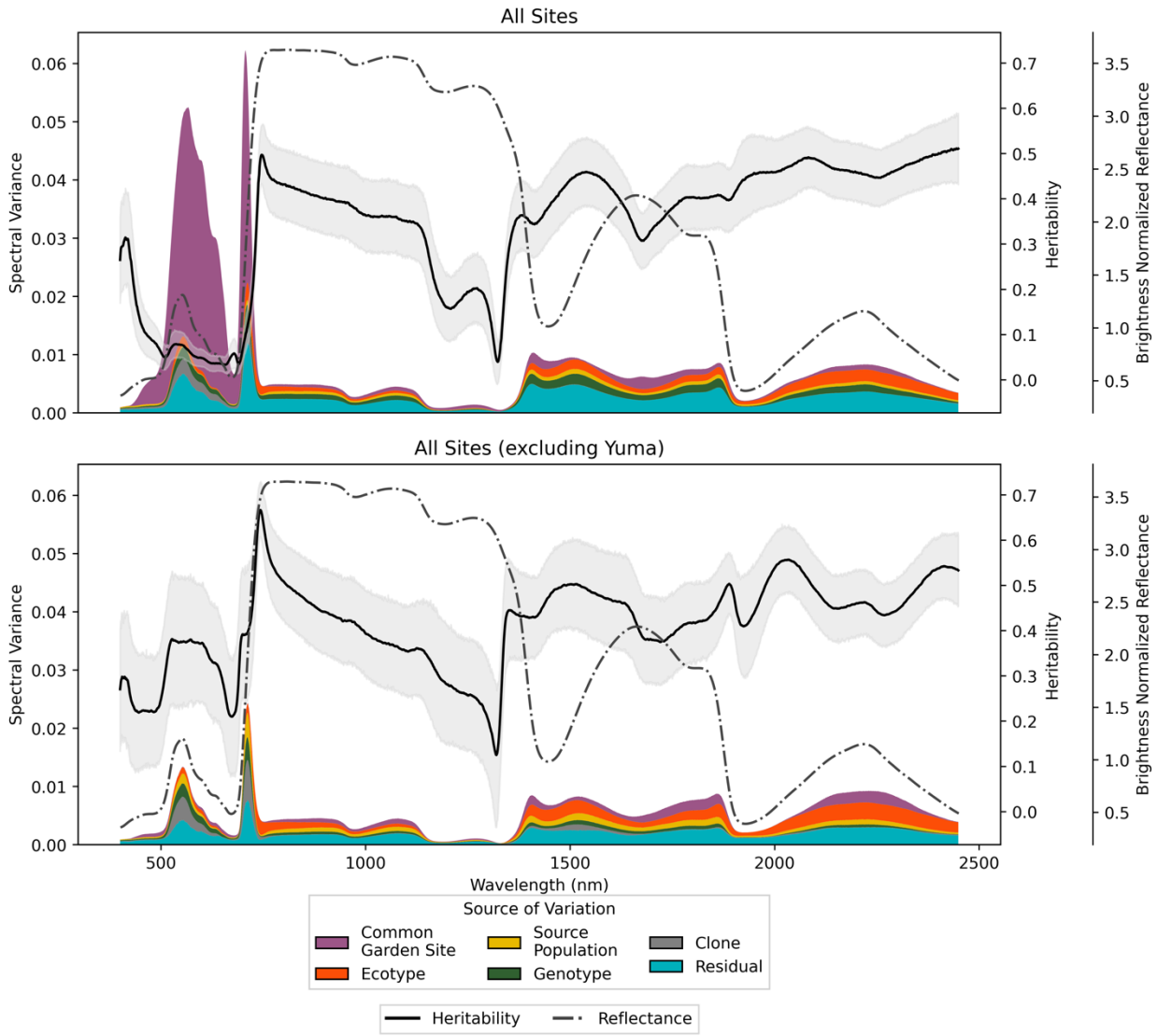

Figure 4: Heritability of reflectance spectra (solid line) and its 95% bootstrapped confidence interval (grey fill), mean brightness normalized reflectance spectra (dotted line), and the source of variability (filled colors) from the visible to shortwave infrared for *Populus fremontii* at a) all sites and b) Canyonlands and Agua Fria. Axes have been scaled to match between plots a and b.

SVM analysis and leaf predictions

SVM models were able to discriminate between spectra based on both common garden site and source population at 96.2% and 78.2% accuracy, respectively (Figure 4). The SVM trained to classify spectra based on the common garden site (environmental variation)

outperformed the SVM trained to discriminate spectra based on source population (genotypic variation). The common garden site SVM accurately predicted spectra from the Yuma site 100% of the time, and confusion in this model occurred primarily between Canyonlands and Agua Fria. The true positive rate for Canyonlands and Agua Fria was 87% and 90%, respectively. For the source population SVM, the true positive rate ranged from 61% for the KWF population to 100% for CLF. The populations that were most often confused were BCE and KWF. When predicting the source population using one common garden site as a holdout for testing, model performance declined. Source populations at Canyonlands were predicted with 35.3% accuracy when trained on data from Agua Fria and Yuma. At Agua Fria and Yuma, accuracy was 36.3% and 16.8%, respectively, when SVM models were trained on data from the other common garden sites. Lastly, we tested the separability of ecotypes at Agua Fria and Canyonlands using an SVM to support the PCA results (Figure 3b). We found that the SVM predicted ecotype with a 76.1% accuracy. Spectra from the Colorado Plateau were less likely to be confused with those from one of the Sonoran Desert ecotypes (Figure S2).

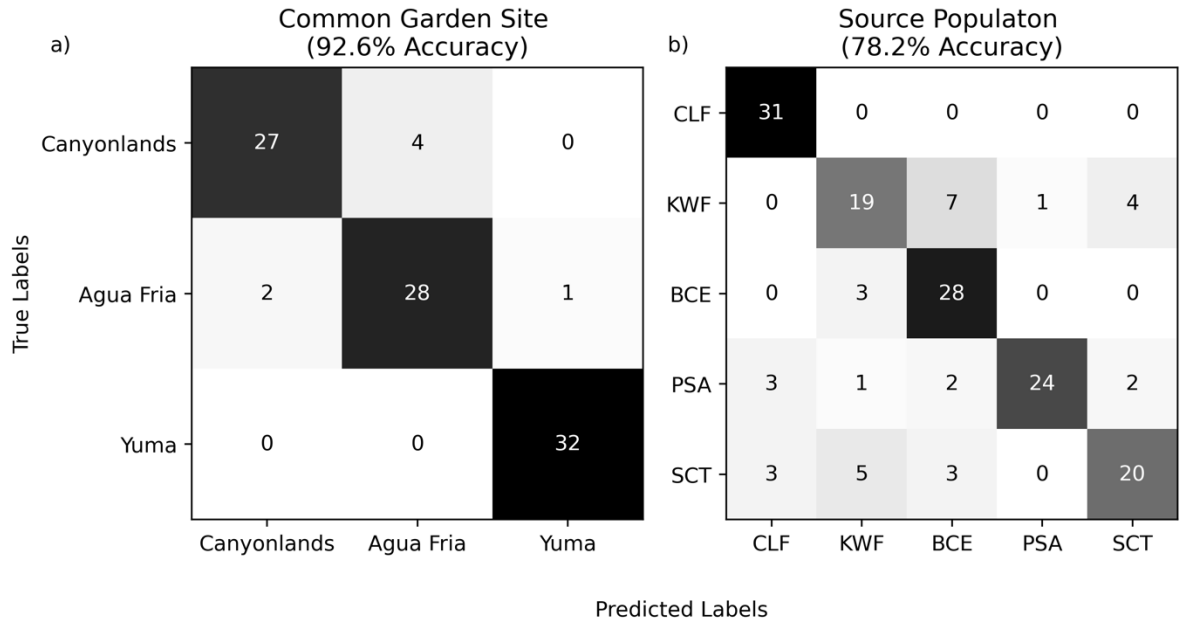

Figure 5: Support vector machine confusion matrix results for predicting a) common garden site and b) source population. Source populations are ordered left to right and top to bottom from lowest to highest mean annual temperature.

Discussion

Reflectance spectra of *P. fremontii* responded to both common garden site and source population, demonstrating that spectra are both plastic and heritable. The degree of plasticity depended on site conditions, with extreme temperatures at Yuma likely causing a threshold change in spectral expression. Here, we defined extreme temperature as the point where the ambient temperatures are at the upper threshold of the *P. fremontii* thermal tolerance (Moran et al., 2023). Heritability and plasticity were displayed across different regions of the leaf reflectance spectrum. This information was used to retrieve genotypic and environmental information from *P. fremontii* individuals at high accuracy using leaf spectroscopy and SVM models.

Heritability and plasticity of reflectance spectra

P. fremontii reflectance demonstrated both plastic (responsive to common garden site) and genotypic responses. The degree of plasticity exhibited by the spectra was significantly influenced by the inclusion of leaf spectra from Yuma. In the first PCA analysis, the first two PCs primarily separated the spectra according to whether the leaves were collected at Yuma or not, likely due to the extreme heat experienced by the trees at Yuma. Similarly, Li et al. (2023) examined genetic variation of *Nicotiana attenuata* (wilt tobacco) across common garden sites in Arizona and Utah, and they found that PC1 of the spectra was primarily influenced by the location of the common garden. *Nicotiana attenuata* genotype affected clustering of PC 2-4, indicating that environment had the primary effect on leaf reflectance while genotype had a secondary effect (Li et al., 2023). In our experiment, the effect of the common garden site depended on the extremity of the environmental conditions, as reflectance was primarily driven by the common garden site only when Yuma was included. Note that this site is near the southern edge of the species' distribution where it may not survive future climatic conditions (e.g., Blasini et al., 2021; Moran et al., 2023).

Excluding Yuma in the second PCA resulted in source population (genotype) being the primary driver of separability, observed by the separation of the Sonoran Desert and Colorado Plateau ecotypes in PC-space. Within the Sonoran Desert group, the two Sonoran Desert ecotypes were separated first by common garden site (environment) and secondly by ecotype (genotype) along the x-axis, showing that reflectance spectra can reveal the nested effects of

genotype and environment on phenotypic variation. In the same study system, Cooper et al. (2019) found that phenotypic plasticity in *P. fremontii* was greater in populations from warmer climates than those from cooler climates, demonstrating that plasticity can also have a genetic component. Further, Corbin et al. (2024) found that, in these same *P. fremontii* common gardens, spectral indices indicative of stress were positively related to the distance trees were moved from their historical climate regardless of whether the trees were moved from warmer to cooler climates or vice versa

The separation of Yuma leaf spectra from Agua Fria or Canyonlands leaf spectra was largely driven by responses in the visible (~450-680 nm) and red-edge (~680-750 nm) portion of the spectra. While this resulted in lower heritability in those wavelengths when Yuma was included, the heritability in green channels increased when Yuma was excluded from the analysis. Heritability in the visible region has been documented in other species (Čepl et al., 2018; Feng et al., 2017; McManus et al., 2016; Seeley, Stacy, Martin, et al., 2023; Tirado et al., 2021). For example, Matsuda et al. found that the reflectance of *Arabidopsis* mutants with altered leaf pigment status differed in the visible range (2012). Similarly, Seeley, Stacy, Martin, & Asner (2023) demonstrated a divergence in chlorophyll content, which was associated with differences in the visible wavelengths, between *Metrosideros polymorpha* varieties that organize along environmental gradients.

Here, we observed a peak in heritability at the red edge, though this peak was narrower and shifted toward longer wavelengths when Yuma was included in the analysis. Both visible and red-edge wavelengths are responsive to stress, and the relative reduction in heritability in these regions caused by Yuma is likely indicative of thermal stress, as discussed in the following section. The heritability of these regions was high relative to the rest of the VSWIR spectra when the extreme stress response was absent, supporting other studies that have observed genetic signals in the red edge. For example, Feng et al. (2017) found that the red edge was predictive of rice genotypes, and both Čepal et al. (2018) and Czyż et al. (2020) observed a red edge signal in the heritability of *Pinus sylvestris* (Scotts pine) and *Fagus sylvatica* (European beech) leaf reflectance, respectively.

Heritability in *P. fremontii* in the NIR peaked at 750 and 1350 nm. These heritability peaks are similar to those of both *Pinus sylvestris* and *F. sylvatica* (Čepl et al., 2018; Czyż et al., 2020), though *Pinus sylvestris* had an additional region of high heritability around 1130-1330 in

the NIR that corresponded to low heritability in *P. fremontii*. As much of the NIR corresponds to leaf structure (Knipling, 1970; Slaton et al., 2001), differences in heritability between *P. fremontii* and *Pinus sylvestris* may relate to differences between broad and needle leaves.

Overall, heritability in the SWIR was high relative to other wavelengths, especially when Yuma was included in the analysis. Spectral variation due to source population and genotype (genetic factors) was greater than variation stemming from common garden sites (environmental factors) across the NIR and SWIR, regardless of the inclusion of Yuma. When predicting the genetic structure of *F. sylvatica* using the airborne prism experiment imaging spectrometer, longer wavelengths (> ~1900nm) in the SWIR were more predictive (Czyż et al., 2020). Yet this region was slightly less important when estimating the heritability of *Pinus sylvestris* (Čepl et al., 2018). McManus et al. (2016) likewise found that the phylogenetic signal was greatest in the SWIR across many Neotropical tree species. Many plant traits such as lignin, cellulose, and tannins are primarily expressed in the SWIR (Asner and Martin, 2016, 2009; Martin et al., 2018), suggesting that plant traits not directly related to photosynthesis may be driving, in part, phylogenetic signals in reflectance spectra.

Utilizing these differences in plasticity and heritability across the spectrum, SVM models were able to separate leaf spectra based on their common garden site and source population with high (>76%) accuracy. Models based on common garden sites were ~14% more accurate than those separating source population spectra, again demonstrating that spectral plasticity linked to heat stress can decrease spectral heritability, especially in extreme environments. Cavender-Bares et al. similarly found that while the source population of *Quercus oleoides* could be distinguished using PLS-DA models (kappa score = 0.342), watering treatment was predicted with greater accuracy (kappa score = 0.61) (2016).

While environmental conditions may exert stronger controls over phenotypic variation between spectra, especially in extreme environments, the retrieval of genetic information is a valuable tool. Phylogenetic organization of reflectance spectra has been observed in Kauai rainforest species (Asner and Martin, 2009), Neotropical tree communities (McManus et al., 2016), *Quercus* species (Cavender-Bares et al., 2016), and grassland-savannah perennial species (Schweiger et al., 2018). Disentangling genotypic versus environmental sources of spectral variation is vital for developing remote sensing methods that can distinguish phenotypic plasticity (the capacity of a single genotype to generate alternative phenotypes based on

environmental conditions; (Arnold et al., 2019), which is an important mechanism of response to global change (Bonamour et al., 2019). As a wide-ranging riparian species with genomic variation shaped by local environmental conditions (Blasini et al., 2021; Bothwell et al., 2023; Erica Sukovich, 2021), *P. fremontii* serves as a case study of how reflectance spectra can be used to understand how climate-driven selection may interact with current climate change (Cooper et al. 2022) to affect a population's persistence on the landscape.

Environmental thresholds

In this common garden study, the extreme temperature at the Yuma site induced a shift in the reflectance spectra. When exposed to extreme heat, plants employ a variety of mechanisms to increase their tolerance. While range shifts are a population-level strategy for plants to survive extreme heat (Bertrand et al., 2011; Lenoir and Svenning, 2015; Walther et al., 2005), plastic responses at the individual level include increased LMA (observed at Yuma), increased heat shock proteins (HSP) to help repair heat damage, concentrations of which have been found to correlate with LMA (Knight and Ackerly, 2003), trichome development to promote self-shading, (Banowetz et al., 2008), an accumulation of phenolics and isoprenoids for their ability to protect photosynthetic apparatuses and antioxidant properties (Ahmad and Prasad, 2011; Bartwal et al., 2013; Smirnoff, 2005), and an increased production of soluble sugars (Liu et al., 2011; Sasaki et al., 1996; Wahid and Close, 2007; Wang et al., 2013) and saturated fatty acids (Ahmad and Prasad, 2011; Tang et al., 2016). As many of these physical and chemical changes such as increased LMA, plant phenols, soluble sugars, and fatty acids can be estimated using spectroscopy (Akkaya, 2018; Asner and Martin, 2016, 2009), it is unsurprising that *P. fremontii* at Yuma differed spectrally from those at the other sites. For *Panax ginseng*, differences between VSWIR reflectance of heat-stressed and control plants corresponded to spectral regions linked to fatty acids, sugars, protein, chlorophyll, and nitrogen (Park et al., 2021). Similarly, other studies have found differences between control and heat-stressed plants using fluorescence (Faqeerzada et al., 2023; Poobalasubramanian et al., 2022) and visible-NIR (Kim et al., 2022) spectroscopy. Further, Serbin et al. (2012) estimated temperature-responsive traits at the landscape scale using imaging spectroscopy data.

The shift in reflectance spectra between the Yuma trees and leaves at the cooler sites primarily occurred in the visible and red-edge wavelengths, indicating that photosystems were

likely disrupted. Together, the visible and red edges are predictive of chlorophyll and other photosynthetic pigments (Horler et al., 1983; Martin et al., 2018; Vogelmann et al., 1993). Both as a mechanism of photosynthetic apparatus protection and as a side effect of stress response, trees at Yuma had higher reflectance in the visible range, similar to that of heat-stressed rice (Xie et al., 2019) and maize (Tirado et al., 2021). As photosystem II is vulnerable to heat, photosynthesis is often the first mechanism influenced by temperature (Berry and Bjorkman, 1980; Mathur et al., 2014). Shifts in the red edge have been linked to plant stressors such as heat and water stress (Dobrowski et al., 2005), bark beetles (Abdullah et al., 2019), and natural gas leakage (Smith et al., 2004), all of which induced changes in chlorophyll (Carter, 1993; Carter and Miller, 1994). The PRI, a plant stress indicator (Thénot et al., 2002), as well as the observed stunted growth of trees at Yuma compared to that at the other sites, supports the conclusion that trees at Yuma were more stressed than those at the other sites.

While the magnitude of variation was greatest in the visible and red-edge when Yuma was included, site-level responses in the SWIR remained regardless of the inclusion of Yuma. Park et al. (2021) noted the importance of the SWIR for separating heat-stressed and control plants using spectroscopy. Further, temperature-dependent leaf traits of other *Populus* species, *P. tremuloides* and *P. deltoides*, which is closely related to *P. fremontii*, were predictable using wavelengths in visible and SWIR regions (Serbin et al., 2012). Both of these studies linked temperature-related responses in the SWIR with plant traits known to respond to heat stress (Park et al., 2021; Serbin et al., 2012). Here, site-level variation between Agua Fria and Canyonlands was primarily observed in the SWIR and, to a lesser degree, the NIR, emphasizing the importance of using the full spectrum to distinguish between temperature treatments.

Implications of climate change on remote sensing

Given the plastic response of reflectance spectra to temperature, it is important to consider how future climate shifts and environmental variations may impact airborne remote sensing. We found that source population classification accuracies were relatively high when data from all sites were represented in the training dataset (71.2%), but the accuracy declined sharply when data from one site was withheld as a test dataset (<36.4%). Similarly, large-scale species classifications have been challenged by geographic differences in reflectance spectra (Seeley et al., 2024) as *in situ* classifications encountered both heritable and plastic variation. The gap in

prediction accuracy was larger at the Yuma site where extreme temperatures resulted in greater spectral variation than at the other sites. While the use of irrigation systems allowed us to control for site-level differences in water availability, it should be noted that temperature responses are exacerbated by drought as water retention behaviors such as stomatal closure result in higher leaf temperatures (Urban et al., 2017). Therefore, collecting training data across a range of temperature and moisture conditions is recommended to increase model universality.

However, while spectral plasticity linked to heat stress may decrease spectral heritability, environmentally sensitive regions of the spectra offer opportunities to understand physiological responses to extreme temperatures at large scales. While phylogenetic models may decline in accuracy where and when extreme climate events occur, comparing phylogenetic information collected in 'typical' years with spectral changes collected during stress events would yield valuable insights into the heritability and phenological plasticity of populations without the need for translocation experiments.

Conclusions

We have shown that reflectance spectra of *P. fremontii* contain information regarding their site location and source population, displaying plasticity and heritability across different parts of the electromagnetic spectrum. We determined that intraspecific spectral variation was driven by both common garden site and source population, with the primary driver depending on the severity of environmental change and degree of genetic separation between populations. Spectra taken from populations growing at the upper-temperature threshold of *P. fremontii* (Yuma site) demonstrated a large variance in the visible and red-edge wavelengths, corresponding to documented responses to heat stress. Across these regions, spectral heritability was low, with extreme temperatures likely causing a threshold change in spectral expression. Despite this stress response, spectra still contained a heritable component of the spectra, mainly across the NIR and SWIR. This information was used to predict the source population of *P. fremontii* individuals at high accuracy using leaf spectroscopy and machine learning models. Increasing airborne and satellite-based imaging spectroscopy offer important metrics to quantify and understand genotypic versus environmental controls on *P. fremontii* at large scales and quantify the heritable resilience of this important foundation species to a rapidly changing

environment. Such findings represent important tools for identifying the optimal genotypes and populations that could be used to mitigate a given level of climate change in restoration.

Acknowledgments

The common gardens were initially developed under NSF Macrosystems grant DEB 2017877 awarded to GJA, TGW, and KCG. Funding for this research was provided by the NSF MacroSystems grant DEB-1340852 awarded to GJA, TGW, and CED as well as the NSF DEB-1340856 awarded to KRH. Author contributions are as follows. Original idea: CED, ET, GPA; common garden development common gardens: GJA, TGW, KCG, KRH, and HFC; data collection: ET; statistical analysis: MMS, ET, methodology: MMS, ET, CED, BCW; writing the manuscript: MMS, ET. All authors reviewed several drafts and agreed with the final version. The authors have declared that no competing interests exist.

Data Availability

All data files will be made available on the Figshare database upon acceptance of the manuscript at DOI: 10.6084/m9.figshare.25719585.

References

Abdullah, H., Skidmore, A.K., Darvishzadeh, R., Heurich, M., 2019. Timing of red-edge and shortwave infrared reflectance critical for early stress detection induced by bark beetle (Ips typographus, L.) attack. International Journal of Applied Earth Observation and Geoinformation 82, 101900. https://doi.org/10.1016/j.jag.2019.101900

Ahmad, P., Prasad, M.N.V., 2011. Environmental Adaptations and Stress Tolerance of Plants in the Era of Climate Change. Springer Science & Business Media.

Akkaya, M.R., 2018. Prediction of fatty acid composition of sunflower seeds by near-infrared reflectance spectroscopy. J Food Sci Technol 55, 2318–2325. https://doi.org/10.1007/s13197-018-3150-x

Allen, C.D., Macalady, A.K., Chenchouni, H., Bachelet, D., McDowell, N., Vennetier, M., Kitzberger, T., Rigling, A., Breshears, D.D., Hogg, E.H. (Ted), Gonzalez, P., Fensham, R., Zhang, Z., Castro, J., Demidova, N., Lim, J.-H., Allard, G., Running, S.W., Semerci, A., Cobb, N., 2010. A global overview of drought and heat-induced tree mortality reveals

emerging climate change risks for forests. Forest Ecology and Management, Adaptation of Forests and Forest Management to Changing Climate 259, 660–684. https://doi.org/10.1016/j.foreco.2009.09.001

Arnold, P.A., Kruuk, L.E.B., Nicotra, A.B., 2019. How to analyse plant phenotypic plasticity in response to a changing climate. New Phytologist 222, 1235–1241. https://doi.org/10.1111/nph.15656

Asner, G.P., Brodrick, P.G., Anderson, C.B., Vaughn, N.R., Knapp, D.E., Martin, R.E., 2016. Progressive forest canopy water loss during the 2012–2015 California drought. PNAS E249–E255.

Asner, G.P., Jones, M.O., Martin, R.E., Knapp, D.E., Hughes, R.F., 2008. Remote sensing of native and invasive species in Hawaiian forests. Remote Sensing of Environment, Earth Observations for Terrestrial Biodiversity and Ecosystems Special Issue 112, 1912–1926. https://doi.org/10.1016/j.rse.2007.02.043

Asner, G.P., Martin, R.E., 2016. Spectranomics: Emerging science and conservation opportunities at the interface of biodiversity and remote sensing. Global Ecology and Conservation 8, 212–219. https://doi.org/10.1016/j.gecco.2016.09.010

Asner, G.P., Martin, R.E., 2009. Airborne spectranomics: mapping canopy chemical and taxonomic diversity in tropical forests. Frontiers in Ecology and the Environment 7, 269–276. https://doi.org/10.1890/070152

Asner, G.P., Martin, R.E., Anderson, C.B., Knapp, D.E., 2015. Quantifying forest canopy traits: Imaging spectroscopy versus field survey. Remote Sensing of Environment 158, 15–27. https://doi.org/10.1016/j.rse.2014.11.011

Asner, G.P., Martin, R.E., Tupayachi, R., Anderson, C.B., Sinca, F., Carranza-Jiménez, L., Martinez, P., 2014. Amazonian functional diversity from forest canopy chemical assembly. Proceedings of the National Academy of Sciences 111, 5604–5609. https://doi.org/10.1073/pnas.1401181111

Asner, G.P., Martin, R.E., Tupayachi, R., Llactayo, W., 2017. Conservation assessment of the Peruvian Andes and Amazon based on mapped forest functional diversity. Biological Conservation 210, 80–88. https://doi.org/10.1016/j.biocon.2017.04.008

Baldeck, C.A., Colgan, M.S., Féret, J.-B., Levick, S.R., Martin, R.E., Asner, G.P., 2014. Landscape-scale variation in plant community composition of an African savanna from

airborne species mapping. Ecological Applications 24, 84–93. https://doi.org/10.1890/13-0307.1

Balzotti, C.S., Asner, G.P., 2018. Biotic and Abiotic Controls Over Canopy Function and Structure in Humid Hawaiian Forests. Ecosystems 21, 331–348. https://doi.org/10.1007/s10021-017-0151-y

Balzotti, C.S., Asner, G.P., Adkins, E.D., Parsons, E.W., 2020. Spatial drivers of composition and connectivity across endangered tropical dry forests. Journal of Applied Ecology 57, 1593–1604. https://doi.org/10.1111/1365-2664.13632

Banowetz, G.M., Azevedo, M.D., Stout, R., 2008. Morphological adaptations of hot springs panic grass (Dichanthelium lanigunosum var sericeum (Schmoll) to thermal stress. Journal of Thermal Biology 33, 106–116. https://doi.org/10.1016/j.jtherbio.2007.08.006

Bartwal, A., Mall, R., Lohani, P., Guru, S.K., Arora, S., 2013. Role of Secondary Metabolites and Brassinosteroids in Plant Defense Against Environmental Stresses. J Plant Growth Regul 32, 216–232. https://doi.org/10.1007/s00344-012-9272-x

Bates, D., Mächler, M., Bolker, B., Walker, S., 2015. Fitting Linear Mixed-Effects Models Using lme4. Journal of Statistical Software 67, 1–48. https://doi.org/10.18637/jss.v067.i01

Berry, J., Bjorkman, O., 1980. Photosynthetic Response and Adaptation to Temperature in Higher Plants. Annual Review of Plant Physiology 31, 491–543. https://doi.org/10.1146/annurev.pp.31.060180.002423

Bertrand, R., Lenoir, J., Piedallu, C., Riofrío-Dillon, G., de Ruffray, P., Vidal, C., Pierrat, J.-C., Gégout, J.-C., 2011. Changes in plant community composition lag behind climate warming in lowland forests. Nature 479, 517–520. https://doi.org/10.1038/nature10548

Blasini, D.E., Koepke, D.F., Grady, K.C., Allan, G.J., Gehring, C.A., Whitham, T.G., Cushman, S.A., Hultine, K.R., 2021. Adaptive trait syndromes along multiple economic spectra define cold and warm adapted ecotypes in a widely distributed foundation tree species. Journal of Ecology 109, 1298–1318. https://doi.org/10.1111/1365-2745.13557

Blonder, B., Graae, B.J., Greer, B., Haagsma, M., Helsen, K., Kapás, R.E., Pai, H., Rieksta, J., Sapena, D., Still, C.J., Strimbeck, R., 2020. Remote sensing of ploidy level in quaking aspen (Populus tremuloides Michx.). Journal of Ecology 108, 175–188. https://doi.org/10.1111/1365-2745.13296

Boardman, J.W., Green, R.O., 2000. Exploring the spectral variability of the Earth as measured by AVIRIS in 1999.

Bonamour, S., Chevin, L.-M., Charmantier, A., Teplitsky, T., 2019. Phenotypic plasticity in response to climate change: the importance of cue variation. Philosophical Transactions of the Royal Society B 374. https://doi.org/doi.org/10.1098/rstb.2018.0178

Bothwell, H.M., Keith, A.R., Cooper, H.F., Hull, J.B., Andrews, L.V., Wehenkel, C., Hultine, K.R., Gehring, C.A., Cushman, S.A., Whitham, T.G., Allan, G.J., 2023. Microevolutionary Processes in a Foundation Tree Inform Macrosystem Patterns of Community Biodiversity and Structure. Forests 14, 943. https://doi.org/10.3390/f14050943

Braatne, J., Rood, S., Heilman, P., 1996. Life history, ecology, and conservation of riparian cottonwoods in North America. pp. 57–85.

Bradshaw, J.E., 2017. Plant breeding: past, present and future. Euphytica 213, 60. https://doi.org/10.1007/s10681-016-1815-y

Brodrick, P.G., Asner, G.P., 2017. Remotely sensed predictors of conifer tree mortality during severe drought. Environ. Res. Lett. 12, 115013. https://doi.org/10.1088/1748-9326/aa8f55

Buddenbaum, H., Rock, G., Hill, J., Werner, W., 2015. Measuring Stress Reactions of Beech Seedlings with PRI, Fluorescence, Temperatures and Emissivity from VNIR and Thermal Field Imaging Spectroscopy. European Journal of Remote Sensing 48, 263–282. https://doi.org/10.5721/EuJRS20154815

Carter, G.A., 1993. Responses of Leaf Spectral Reflectance to Plant Stress. American Journal of Botany 80, 239–243. https://doi.org/10.1002/j.1537-2197.1993.tb13796.x

Carter, G.A., Miller, R.L., 1994. Early detection of plant stress by digital imaging within narrow stress-sensitive wavebands. Remote Sensing of Environment 50, 295–302. https://doi.org/10.1016/0034-4257(94)90079-5

Cavender-Bares, J., Meireles, J.E., Couture, J.J., Kaproth, M.A., Kingdon, C.C., Singh, A., Serbin, S.P., Center, A., Zuniga, E., Pilz, G., Townsend, P.A., 2016. Associations of Leaf Spectra with Genetic and Phylogenetic Variation in Oaks: Prospects for Remote Detection of Biodiversity. Remote Sensing 8, 221. https://doi.org/10.3390/rs8030221

Čepl, J., Stejskal, J., Lhotáková, Z., Holá, D., Korecký, J., Lstibůrek, M., Tomášková, I., Kočová, M., Rothová, O., Palovská, M., Hejtmánek, J., Krejzková, A., Gezan, S., Whetten, R., Albrechtová, J., 2018. Heritable variation in needle spectral reflectance of Scots pine (Pinus sylvestris L.) peaks in red edge. Remote Sensing of Environment 219, 89–98. https://doi.org/10.1016/j.rse.2018.10.001

Christen, D., Schönmann, S., Jermini, M., Strasser, R.J., Défago, G., 2007. Characterization and early detection of grapevine (Vitis vinifera) stress responses to esca disease by in situ chlorophyll fluorescence and comparison with drought stress. Environmental and Experimental Botany 60, 504–514. https://doi.org/10.1016/j.envexpbot.2007.02.003

Cooper, H.F., Best, R.J., Andrews, L.V., Corbin, J.P.M., Garthwaite, I., Grady, K.C., Gehring, C.A., Hultine, K.R., Whitham, T.G., Allan, G.J., 2022. Evidence of climate-driven selection on tree traits and trait plasticity across the climatic range of a riparian foundation species. Molecular Ecology 31, 5024–5040. https://doi.org/10.1111/mec.16645

Cooper, H.F., Grady, K.C., Cowan, J.A., Best, R.J., Allan, G.J., Whitham, T.G., 2019. Genotypic variation in phenological plasticity: Reciprocal common gardens reveal adaptive responses to warmer springs but not to fall frost. Global Change Biology 25, 187–200. https://doi.org/10.1111/gcb.14494

Cotrozzi, L., 2022. Spectroscopic detection of forest diseases: a review (1970–2020). J. For. Res. 33, 21–38. https://doi.org/10.1007/s11676-021-01378-w

Czyż, E.A., Guillén Escribà, C., Wulf, H., Tedder, A., Schuman, M.C., Schneider, F.D., Schaepman, M.E., 2020. Intraspecific genetic variation of a Fagus sylvatica population in a temperate forest derived from airborne imaging spectroscopy time series. Ecology and Evolution 10, 7419–7430. https://doi.org/10.1002/ece3.6469

Dai, J., Vaughn, N.R., Seeley, M., Heckler, J., Thompson, D.R., Asner, G.P., 2022. Spectral dimensionality of imaging spectroscopy data over diverse landscapes and spatial resolutions. JARS 16, 044518. https://doi.org/10.1117/1.JRS.16.044518

Dalponte, M., Bruzzone, L., Gianelle, D., 2012. Tree species classification in the Southern Alps based on the fusion of very high geometrical resolution multispectral/hyperspectral images and LiDAR data. Remote Sensing of Environment 123, 258–270. https://doi.org/10.1016/j.rse.2012.03.013

Degerickx, J., Roberts, D.A., McFadden, J.P., Hermy, M., Somers, B., 2018. Urban tree health assessment using airborne hyperspectral and LiDAR imagery. International Journal of Applied Earth Observation and Geoinformation 73, 26–38. https://doi.org/10.1016/j.jag.2018.05.021

Dobrowski, S.Z., Pushnik, J.C., Zarco-Tejada, P.J., Ustin, S.L., 2005. Simple reflectance indices track heat and water stress-induced changes in steady-state chlorophyll fluorescence at the canopy scale. Remote Sensing of Environment 97, 403–414. https://doi.org/10.1016/j.rse.2005.05.006

Ellison, A.M., Bank, M.S., Clinton, B.D., Colburn, E.A., Elliott, K., Ford, C.R., Foster, D.R., Kloeppel, B.D., Knoepp, J.D., Lovett, G.M., Mohan, J., Orwig, D.A., Rodenhouse, N.L., Sobczak, W.V., Stinson, K.A., Stone, J.K., Swan, C.M., Thompson, J., Von Holle, B., Webster, J.R., 2005. Loss of foundation species: consequences for the structure and dynamics of forested ecosystems. Frontiers in Ecology and the Environment 3, 479–486. https://doi.org/10.1890/1540-9295(2005)003[0479:LOFSCF]2.0.CO;2

Erica Sukovich, 2021. Molecular Signatures of Selection in Populus fremontii: Precipitation and Temperature as Drivers of Genomic Variation (Thesis). Northern Arizona University.

Faqeerzada, M.A., Park, E., Kim, T., Kim, M.S., Baek, I., Joshi, R., Kim, J., Cho, B.-K., 2023. Fluorescence Hyperspectral Imaging for Early Diagnosis of Heat-Stressed Ginseng Plants. Applied Sciences 13, 31. https://doi.org/10.3390/app13010031

Feng, H., Guo, Z., Yang, W., Huang, C., Chen, G., Fang, W., Xiong, X., Zhang, H., Wang, G., Xiong, L., Liu, Q., 2017. An integrated hyperspectral imaging and genome-wide association analysis platform provides spectral and genetic insights into the natural variation in rice. Sci Rep 7, 4401. https://doi.org/10.1038/s41598-017-04668-8

Féret, J.-B., Asner, G.P., 2014. Mapping tropical forest canopy diversity using high-fidelity imaging spectroscopy. Ecological Applications 24, 1289–1296. https://doi.org/10.1890/13-1824.1

Feret, J.-B., Asner, G.P., 2013. Tree Species Discrimination in Tropical Forests Using Airborne Imaging Spectroscopy. IEEE Transactions on Geoscience and Remote Sensing 51, 73–84. https://doi.org/10.1109/TGRS.2012.2199323

Ferrier, S.M., Bangert, R.K., Hersch-Green, E.I., Bailey, J.K., Allan, G.J., Whitham, T.G., 2012. Unique arthropod communities on different host-plant genotypes results in greater

arthropod diversity. Arthropod-Plant Interactions 6, 187–195. https://doi.org/10.1007/s11829-011-9177-9

Fyllas, N.M., Patiño, S., Baker, T.R., Bielefeld Nardoto, G., Martinelli, L.A., Quesada, C.A., Paiva, R., Schwarz, M., Horna, V., Mercado, L.M., Santos, A., Arroyo, L., Jiménez, E.M., Luizão, F.J., Neill, D.A., Silva, N., Prieto, A., Rudas, A., Silviera, M., Vieira, I.C.G., Lopez-Gonzalez, G., Malhi, Y., Phillips, O.L., Lloyd, J., 2009. Basin-wide variations in foliar properties of Amazonian forest: phylogeny, soils and climate. Biogeosciences 6, 2677–2708. https://doi.org/10.5194/bg-6-2677-200910.5194/bgd-6-3707-2009

Gamon, J.A., Peñuelas, J., Field, C.B., 1992. A narrow-waveband spectral index that tracks diurnal changes in photosynthetic efficiency. Remote Sensing of Environment 41, 35–44. https://doi.org/10.1016/0034-4257(92)90059-S

Glenn, E., Tanner, R., Mendez, S., Kehret, T., Moore, D., Garcia, J., Valdes, C., 1998. Growth rates, salt tolerance and water use characteristics of native and invasive riparian plants from the delta of the Colorado River, Mexico. Journal of Arid Environments 40, 281–294. https://doi.org/10.1006/jare.1998.0443

Grady, K., 2012. Restoration of riparian forests during climate change. Northern Arizona University.

Grady, K.C., Laughlin, D.C., Ferrier, S.M., Kolb, T.E., Hart, S.C., Allan, G.J., Whitham, T.G., 2013. Conservative leaf economic traits correlate with fast growth of genotypes of a foundation riparian species near the thermal maximum extent of its geographic range. Functional Ecology 27, 428–438. https://doi.org/10.1111/1365-2435.12060

Green, R.O., Boardman, J.W., 2000. Exploration of the relationship between information content and signal-to-noise ratio and spatial resolution in AVIRIS spectral data. Spectrum 7.

Hernández-Clemente, R., Navarro-Cerrillo, R.M., Suárez, L., Morales, F., Zarco-Tejada, P.J., 2011. Assessing structural effects on PRI for stress detection in conifer forests. Remote Sensing of Environment 115, 2360–2375. https://doi.org/10.1016/j.rse.2011.04.036

Horler, D.N.H., Dockray, M., Barber, J., 1983. The red edge of plant leaf reflectance. International Journal of Remote Sensing 4, 273–288. https://doi.org/10.1080/01431168308948546

Hühn, M., 1975. Estimation of broad sense heritability in plant populations: an improved method. Theoret. Appl. Genetics 46, 87–99. https://doi.org/10.1007/BF00281647

Hultine, K.R., Allan, G.J., Blasini, D., Bothwell, H.M., Cadmus, A., Cooper, H.F., Doughty, C.E., Gehring, C.A., Gitlin, A.R., Grady, K.C., Hull, J.B., Keith, A.R., Koepke, D.F., Markovchick, L., Corbin Parker, J.M., Sankey, T.T., Whitham, T.G., 2020. Adaptive capacity in the foundation tree species Populus fremontii: implications for resilience to climate change and non-native species invasion in the American Southwest. Conservation Physiology 8, coaa061. https://doi.org/10.1093/conphys/coaa061

Ikeda, D.H., Max, T.L., Allan, G.J., Lau, M.K., Shuster, S.M., Whitham, T.G., 2017. Genetically informed ecological niche models improve climate change predictions. Global Change Biology 23, 164–176. https://doi.org/10.1111/gcb.13470

Kim, G., Lee, H., Wi, S.H., Cho, B.-K., 2022. Snapshot-Based Visible-Near Infrared Multispectral Imaging for Early Screening of Heat Injury during Growth of Chinese Cabbage. Applied Sciences 12, 9340. https://doi.org/10.3390/app12189340

Knight, C.A., Ackerly, D.D., 2003. Evolution and plasticity of photosynthetic thermal tolerance, specific leaf area and leaf size: congeneric species from desert and coastal environments. New Phytologist 160, 337–347. https://doi.org/10.1046/j.1469-8137.2003.00880.x

Knipling, E.B., 1970. Physical and physiological basis for the reflectance of visible and near-infrared radiation from vegetation. Remote Sensing of Environment 1, 155–159. https://doi.org/10.1016/S0034-4257(70)80021-9

Kohzuma, K., Tamaki, M., Hikosaka, K., 2021. Corrected photochemical reflectance index (PRI) is an effective tool for detecting environmental stresses in agricultural crops under light conditions. J Plant Res 134, 683–694. https://doi.org/10.1007/s10265-021-01316-1

Kruse, F.A., Heidebrecht, K.B., Shapiro, A.T., Barloon, P.J., Goetz, A.F.H., 1993. The Spectral Image Processing System (SIPS) Interactive Visualization and Analysis of Imaging Spectrometer Data. Remote Sensing of Environment 44, 145–163.

Laitinen, R.A.E., Nikoloski, Z., 2019. Genetic basis of plasticity in plants. Journal of Experimental Botany 70, 739–745. https://doi.org/10.1093/jxb/ery404

Lenoir, J., Svenning, J.-C., 2015. Climate-related range shifts – a global multidimensional synthesis and new research directions. Ecography 38, 15–28. https://doi.org/10.1111/ecog.00967

Li, C., Czyż, E.A., Halitschke, R., Baldwin, I.T., Schaepman, M.E., Schuman, M.C., 2023. Evaluating potential of leaf reflectance spectra to monitor plant genetic variation. Plant Methods 19, 108. https://doi.org/10.1186/s13007-023-01089-9

Liu, X., Wang, L., Liu, L., Guo, Y., Ren, H., 2011. Alleviating effect of exogenous nitric oxide in cucumber seedling against chilling stress. African Journal of Biotechnology 10, 4380–4386.

Madritch, M.D., Kingdon, C.C., Singh, A., Mock, K.E., Lindroth, R.L., Townsend, P.A., 2014. Imaging spectroscopy links aspen genotype with below-ground processes at landscape scales. Philos Trans R Soc Lond B Biol Sci 369. https://doi.org/10.1098/rstb.2013.0194

Martin, R.E., Chadwick, K.D., Brodrick, P.G., Carranza-Jimenez, L., Vaughn, N.R., Asner, G.P., 2018. An Approach for Foliar Trait Retrieval from Airborne Imaging Spectroscopy of Tropical Forests. Remote Sensing 10, 199. https://doi.org/10.3390/rs10020199

Mathur, S., Agrawal, D., Jajoo, A., 2014. Photosynthesis: Response to high temperature stress. Journal of Photochemistry and Photobiology B: Biology, Stress and Photosynthesis 137, 116–126. https://doi.org/10.1016/j.jphotobiol.2014.01.010

Matsuda, O., Tanaka, A., Fujita, T., Iba, K., 2012. Hyperspectral Imaging Techniques for Rapid Identification of Arabidopsis Mutants with Altered Leaf Pigment Status. Plant and Cell Physiology 53, 1154–1170. https://doi.org/10.1093/pcp/pcs043

McManus, K.M., Asner, G.P., Martin, R.E., Dexter, K.G., Kress, W.J., Field, C.B., 2016. Phylogenetic Structure of Foliar Spectral Traits in Tropical Forest Canopies. Remote Sensing 8, 196. https://doi.org/10.3390/rs8030196

Melgani, F., Bruzzone, L., 2004. Classification of hyperspectral remote sensing images with support vector machines. IEEE Transactions on Geoscience and Remote Sensing 42, 1778–1790. https://doi.org/10.1109/TGRS.2004.831865

Moran, M.E., Aparecido, L.M.T., Koepke, D.F., Cooper, H.F., Doughty, C.E., Gehring, C.A., Throop, H.L., Whitham, T.G., Allan, G.J., Hultine, K.R., 2023. Limits of thermal and hydrological tolerance in a foundation tree species (Populus fremontii) in the desert southwestern United States. New Phytologist 240, 2298–2311. https://doi.org/10.1111/nph.19247

Munaiz, E.D., Townsend, P.A., Havey, M.J., 2020. Reflectance Spectroscopy for Non-Destructive Measurement and Genetic Analysis of Amounts and Types of Epicuticular

Waxes on Onion Leaves. Molecules 25, 3454. https://doi.org/10.3390/molecules25153454

Myneni, R.B., Ross, J., Asrar, G., 1989. A review on the theory of photon transport in leaf canopies. Agricultural and Forest Meteorology 45, 1–153. https://doi.org/10.1016/0168-1923(89)90002-6

Nagler, P., Jetton, A., Fleming, J., Didan, K., Glenn, E., Erker, J., Morino, K., Milliken, J., Gloss, S., 2007. Evapotranspiration in a cottonwood (*Populus fremontii*) restoration plantation estimated by sap flow and remote sensing methods. Agricultural and Forest Meteorology 144, 95–110. https://doi.org/10.1016/j.agrformet.2007.02.002

O'Neill, B.C., Oppenheimer, M., Warren, R., Hallegatte, S., Kopp, R.E., Pörtner, H.O., Scholes, R., Birkmann, J., Foden, W., Licker, R., Mach, K.J., Marbaix, P., Mastrandrea, M.D., Price, J., Takahashi, K., van Ypersele, J.-P., Yohe, G., 2017. IPCC reasons for concern regarding climate change risks. Nature Clim Change 7, 28–37. https://doi.org/10.1038/nclimate3179

Pachauri, R.K., Allen, M.R., Barros, V.R., Broome, J., Cramer, W., Christ, R., Church, J.A., Clarke, L., Dahe, Q., Dasgupta, P., Dubash, N.K., Edenhofer, O., Elgizouli, I., Field, C.B., Forster, P., Friedlingstein, P., Fuglestvedt, J., Gomez-Echeverri, L., Hallegatte, S., Hegerl, G., Howden, M., Jiang, K., Jimenez Cisneroz, B., Kattsov, V., Lee, H., Mach, K.J., Marotzke, J., Mastrandrea, M.D., Meyer, L., Minx, J., Mulugetta, Y., O'Brien, K., Oppenheimer, M., Pereira, J.J., Pichs-Madruga, R., Plattner, G.-K., Pörtner, H.-O., Power, S.B., Preston, B., Ravindranath, N.H., Reisinger, A., Riahi, K., Rusticucci, M., Scholes, R., Seyboth, K., Sokona, Y., Stavins, R., Stocker, T.F., Tschakert, P., van Vuuren, D., van Ypserle, J.-P., 2014. Climate Change 2014: Synthesis Report. Contribution of Working Groups I, II and III to the Fifth Assessment Report of the Intergovernmental Panel on Climate Change, EPIC3Geneva, Switzerland, IPCC, 151 p., pp. 151, ISBN: 978-92-9169-143-2. IPCC, Geneva, Switzerland.

Park, E., Kim, Y.-S., Omari, M.K., Suh, H.-K., Faqeerzada, M.A., Kim, M.S., Baek, I., Cho, B.-K., 2021. High-Throughput Phenotyping Approach for the Evaluation of Heat Stress in Korean Ginseng (Panax ginseng Meyer) Using a Hyperspectral Reflectance Image. Sensors 21, 5634. https://doi.org/10.3390/s21165634

Pedregosa, F., Varoquaux, G., Gramfort, A., Michel, V., Thirion, B., Grisel, O., Blondel, M., Prettenhofer, P., Weiss, R., Dubourg, V., Vanderplas, J., Passos, A., Cournapeau, D., Brucher, M., Perrot, M., Duchesnay, É., 2011. Scikit-learn: Machine Learning in Python. Journal of Machine Learning Research 12, 2825–2830.

Pengra, B.W., Johnston, C.A., Loveland, T.R., 2007. Mapping an invasive plant, Phragmites australis, in coastal wetlands using the EO-1 Hyperion hyperspectral sensor. Remote Sensing of Environment 108, 74–81. https://doi.org/10.1016/j.rse.2006.11.002

Pimm, S.L., Jenkins, C.N., Abell, R., Brooks, T.M., Gittleman, J.L., Joppa, L.N., Raven, P.H., Roberts, C.M., Sexton, J.O., 2014. The biodiversity of species and their rates of extinction, distribution, and protection. Science 344, 1246752. https://doi.org/10.1126/science.1246752

Poobalasubramanian, M., Park, E.-S., Faqeerzada, M.A., Kim, T., Kim, M.S., Baek, I., Cho, B.-K., 2022. Identification of Early Heat and Water Stress in Strawberry Plants Using Chlorophyll-Fluorescence Indices Extracted via Hyperspectral Images. Sensors 22, 8706. https://doi.org/10.3390/s22228706

Roberts, D.A., Dennison, P.E., Gardner, M.E., Hetzel, Y., Ustin, S.L., Lee, C.T., 2003. Evaluation of the potential of Hyperion for fire danger assessment by comparison to the Airborne Visible/Infrared Imaging Spectrometer. IEEE Transactions on Geoscience and Remote Sensing 41, 1297–1310. https://doi.org/10.1109/TGRS.2003.812904

Rose, R.A., Byler, D., Eastman, J.R., Fleishman, E., Geller, G., Goetz, S., Guild, L., Hamilton, H., Hansen, M., Headley, R., Hewson, J., Horning, N., Kaplin, B.A., Laporte, N., Leidner, A., Leimgruber, P., Morisette, J., Musinsky, J., Pintea, L., Prados, A., Radeloff, V.C., Rowen, M., Saatchi, S., Schill, S., Tabor, K., Turner, W., Vodacek, A., Vogelmann, J., Wegmann, M., Wilkie, D., Wilson, C., 2015. Ten ways remote sensing can contribute to conservation. Conservation Biology 29, 350–359. https://doi.org/10.1111/cobi.12397

Rossini, M., Fava, F., Cogliati, S., Meroni, M., Marchesi, A., Panigada, C., Giardino, C., Busetto, L., Migliavacca, M., Amaducci, S., Colombo, R., 2013. Assessing canopy PRI from airborne imagery to map water stress in maize. ISPRS Journal of Photogrammetry and Remote Sensing 86, 168–177. https://doi.org/10.1016/j.isprsjprs.2013.10.002

Rull, V., Vegas-Vilarrúbia, T., 2006. Unexpected biodiversity loss under global warming in the neotropical Guayana Highlands: a preliminary appraisal. Global Change Biology 12, 1–9. https://doi.org/10.1111/j.1365-2486.2005.001080.x

Sampaio, P.S., Castanho, A., Almeida, A.S., Oliveira, J., Brites, C., 2020. Identification of rice flour types with near-infrared spectroscopy associated with PLS-DA and SVM methods. Eur Food Res Technol 246, 527–537. https://doi.org/10.1007/s00217-019-03419-5

Sasaki, H., Ichimura, K., Oda, M., 1996. Changes in Sugar Content during Cold Acclimation and Deacclimation of Cabbage Seedlings. Annals of Botany 78, 365–369. https://doi.org/10.1006/anbo.1996.0131

Scheiner, S.M., 1993. Genetics and Evolution of Phenotypic Plasticity. Annual Review of Ecology, Evolution, and Systematics 24, 35–68. https://doi.org/10.1146/annurev.es.24.110193.000343

Schweiger, A.K., Cavender-Bares, J., Townsend, P.A., Hobbie, S.E., Madritch, M.D., Wang, R., Tilman, D., Gamon, J.A., 2018. Plant spectral diversity integrates functional and phylogenetic components of biodiversity and predicts ecosystem function. Nat Ecol Evol 2, 976–982. https://doi.org/10.1038/s41559-018-0551-1

Schweiger, R., Kaufman, S., Laaksonen, R., Kleber, M.E., März, W., Eskin, E., Rosset, S., Halperin, E., 2016. Fast and Accurate Construction of Confidence Intervals for Heritability. Am J Hum Genet 98, 1181–1192. https://doi.org/10.1016/j.ajhg.2016.04.016

Seeley, M., Asner, G.P., 2021. Imaging Spectroscopy for Conservation Applications. Remote Sensing 13, 292. https://doi.org/10.3390/rs13020292

Seeley, Megan M., Martin, R.E., Giardina, C., Luiz, B., Francisco, K., Cook, Z., Hughes, M.A., Asner, G.P., 2023a. Leaf spectroscopy of resistance to Ceratocystis wilt of ‘Ōhi’a. PLOS ONE 18, e0287144. https://doi.org/10.1371/journal.pone.0287144

Seeley, Megan M., Martin, R.E., Vaughn, N.R., Thompson, D.R., Dai, J., Asner, G.P., 2023b. Quantifying the Variation in Reflectance Spectra of Metrosideros polymorpha Canopies across Environmental Gradients. Remote Sensing 15, 1614. https://doi.org/10.3390/rs15061614

Seeley, M. M., Stacy, E.A., Martin, R.E., Asner, G.P., 2023. Foliar functional and genetic variation in a keystone Hawaiian tree species estimated through spectroscopy. Oecologia. https://doi.org/10.1007/s00442-023-05374-1

Seeley, M M, Vaughn, N.R., Asner, G.A., 2023. Evaluating individual tree species classification performance across diverse environments. Environ. Res.: Ecology 3, 011001. https://doi.org/10.1088/2752-664X/ad1f49

Seeley, M.M., Vaughn, N.R., Asner, G.P., 2024. Evaluating individual tree species classification performance across diverse environments. Environmental Research: Ecology 3, 011001.

Seeley, Megan M., Vaughn, N.R., Shanks, B.L., Martin, R.E., König, M., Asner, G.P., 2023c. Classifying a highly polymorphic tree species across landscapes using airborne imaging spectroscopy. Remote Sensing 15, 4365. https://doi.org/10.3390/rs15184365

Serbin, S.P., Dillaway, D.N., Kruger, E.L., Townsend, P.A., 2012. Leaf optical properties reflect variation in photosynthetic metabolism and its sensitivity to temperature. Journal of Experimental Botany 63, 489–502. https://doi.org/10.1093/jxb/err294

Shafroth, P.B., Friedman, J.M., Ischinger, L.S., 1995. Effects of Salinity on Establishment of Populus Fremontii (cottonwood) and Tamarix Ramosissima (saltcedar) in Southwestern United States. The Great Basin Naturalist 55, 58–65.

Shendryk, I., Broich, M., Tulbure, M.G., McGrath, A., Keith, D., Alexandrov, S.V., 2016. Mapping individual tree health using full-waveform airborne laser scans and imaging spectroscopy: A case study for a floodplain eucalypt forest. Remote Sensing of Environment 187, 202–217. https://doi.org/10.1016/j.rse.2016.10.014

Skowronek, S., Asner, G.P., Feilhauer, H., 2017. Performance of one-class classifiers for invasive species mapping using airborne imaging spectroscopy. Ecological Informatics 37, 66–76. https://doi.org/10.1016/j.ecoinf.2016.11.005

Slaton, M.R., Raymond Hunt Jr., E., Smith, W.K., 2001. Estimating near-infrared leaf reflectance from leaf structural characteristics. American Journal of Botany 88, 278–284. https://doi.org/10.2307/2657019

Smirnoff, N., 2005. Antioxidants and Reactive Oxygen Species in Plants. John Wiley & Sons, Ltd. https://doi.org/10.1002/9780470988565.fmatter

Smith, K.L., Steven, M.D., Colls, J.J., 2004. Use of hyperspectral derivative ratios in the red-edge region to identify plant stress responses to gas leaks. Remote Sensing of Environment 92, 207–217. https://doi.org/10.1016/j.rse.2004.06.002

Somers, B., Asner, G.P., 2013. Invasive Species Mapping in Hawaiian Rainforests Using Multi-Temporal Hyperion Spaceborne Imaging Spectroscopy. IEEE Journal of Selected Topics

in Applied Earth Observations and Remote Sensing 6, 351–359. https://doi.org/10.1109/JSTARS.2012.2203796

Stromberg, J., 1998. Dynamics of Fremont cottonwood (*Populus fremontii*) and saltcedar (*Tamarix chinensis*) populations along the San Pedro River, Arizona. Journal of Arid Environments 40, 133–155. https://doi.org/10.1006/jare.1998.0438

Stromberg, J.C., 2001. Restoration of riparian vegetation in the south-western United States: importance of flow regimes and fluvial dynamism. Journal of Arid Environments 49, 17–34. https://doi.org/10.1006/jare.2001.0833

Suárez, L., Zarco-Tejada, P.J., González-Dugo, V., Berni, J.A.J., Sagardoy, R., Morales, F., Fereres, E., 2010. Detecting water stress effects on fruit quality in orchards with time-series PRI airborne imagery. Remote Sensing of Environment 114, 286–298. https://doi.org/10.1016/j.rse.2009.09.006

Tang, T., Liu, P., Zheng, G., Li, W., 2016. Two phases of response to long-term moderate heat: Variation in thermotolerance between Arabidopsis thaliana and its relative Arabis paniculata. Phytochemistry 122, 81–90. https://doi.org/10.1016/j.phytochem.2016.01.003

Thai, H.-T., Mentré, F., Holford, N.H.G., Veyrat-Follet, C., Comets, E., 2013. A comparison of bootstrap approaches for estimating uncertainty of parameters in linear mixed-effects models. Pharmaceutical Statistics 12, 129–140. https://doi.org/10.1002/pst.1561

Thénot, F., Méthy, M., Winkel, T., 2002. The Photochemical Reflectance Index (PRI) as a water-stress index. International Journal of Remote Sensing - INT J REMOTE SENS 23, 5135–5139. https://doi.org/10.1080/01431160210163100

Thomas, C.D., Cameron, A., Green, R.E., Bakkenes, M., Beaumont, L.J., Collingham, Y.C., Erasmus, B.F.N., de Siqueira, M.F., Grainger, A., Hannah, L., Hughes, L., Huntley, B., van Jaarsveld, A.S., Midgley, G.F., Miles, L., Ortega-Huerta, M.A., Townsend Peterson, A., Phillips, O.L., Williams, S.E., 2004. Extinction risk from climate change. Nature 427, 145–148. https://doi.org/10.1038/nature02121

Thompson, D.R., Boardman, J.W., Eastwood, M.L., Green, R.O., 2017. A large airborne survey of Earth's visible-infrared spectral dimensionality. Opt. Express 25, 9186. https://doi.org/10.1364/OE.25.009186

Tirado, S.B., Dennis, S.St., Enders, T.A., Springer, N.M., 2021. Utilizing spatial variability from hyperspectral imaging to assess variation in maize seedlings. The Plant Phenome Journal 4, e20013. https://doi.org/10.1002/ppj2.20013

Torabzadeh, H., Leiterer, R., Hueni, A., Schaepman, M.E., Morsdorf, F., 2019. Tree species classification in a temperate mixed forest using a combination of imaging spectroscopy and airborne laser scanning. Agricultural and Forest Meteorology 279, 107744. https://doi.org/10.1016/j.agrformet.2019.107744

Townsend, P.A., Foster, J.R., Chastain, R.A., Currie, W.S., 2003. Application of imaging spectroscopy to mapping canopy nitrogen in the forests of the central Appalachian Mountains using Hyperion and AVIRIS. IEEE Transactions on Geoscience and Remote Sensing 41, 1347–1354. https://doi.org/10.1109/TGRS.2003.813205

Turner, M., 2023. Heritable trait variation for climate resilience. Nat Ecol Evol 7, 492–492. https://doi.org/10.1038/s41559-023-02004-0

Turner, W., Spector, S., Gardiner, N., Fladeland, M., Sterling, E., Steininger, M., 2003. Remote sensing for biodiversity science and conservation. Trends in Ecology & Evolution 18, 306–314. https://doi.org/10.1016/S0169-5347(03)00070-3

Urban, J., Ingwers, M.W., McGuire, M.A., Teskey, R.O., 2017. Increase in leaf temperature opens stomata and decouples net photosynthesis from stomatal conductance in Pinus taeda and Populus deltoides x nigra. Journal of Experimental Botany 68, 1757–1767. https://doi.org/10.1093/jxb/erx052

Ustin, S.L., Gamon, J.A., 2010. Remote sensing of plant functional types. New Phytologist 186, 795–816. https://doi.org/10.1111/j.1469-8137.2010.03284.x

Vahsen, M.L., Blum, M.J., Megonigal, J.P., Emrich, S.J., Holmquist, J.R., Stiller, B., Todd-Brown, K.E.O., McLachlan, J.S., 2023. Rapid plant trait evolution can alter coastal wetland resilience to sea level rise. Science 379, 393–398. https://doi.org/10.1126/science.abq0595

Vaughn, N.R., Asner, G.P., Brodrick, P.G., Martin, R.E., Heckler, J.W., Knapp, D.E., Hughes, R.F., 2018. An Approach for High-Resolution Mapping of Hawaiian Metrosideros Forest Mortality Using Laser-Guided Imaging Spectroscopy. Remote Sensing 10, 502. https://doi.org/10.3390/rs10040502

Virtanen, P., Gommers, R., Oliphant, T.E., Haberland, M., Reddy, T., Cournapeau, D., Burovski, E., Peterson, P., Weckesser, W., Bright, J., van der Walt, S.J., Brett, M., Wilson, J., Millman, K.J., Mayorov, N., Nelson, A.R.J., Jones, E., Kern, R., Larson, E., Carey, C.J., Polat, İ., Feng, Y., Moore, E.W., VanderPlas, J., Laxalde, D., Perktold, J., Cimrman, R., Henriksen, I., Quintero, E.A., Harris, C.R., Archibald, A.M., Ribeiro, A.H., Pedregosa, F., van Mulbregt, P., SciPy 1.0 Contributors, Vijaykumar, A., Bardelli, A.P., Rothberg, A., Hilboll, A., Kloeckner, A., Scopatz, A., Lee, A., Rokem, A., Woods, C.N., Fulton, C., Masson, C., Häggström, C., Fitzgerald, C., Nicholson, D.A., Hagen, D.R., Pasechnik, D.V., Olivetti, E., Martin, E., Wieser, E., Silva, F., Lenders, F., Wilhelm, F., Young, G., Price, G.A., Ingold, G.-L., Allen, G.E., Lee, G.R., Audren, H., Probst, I., Dietrich, J.P., Silterra, J., Webber, J.T., Slavič, J., Nothman, J., Buchner, J., Kulick, J., Schönberger, J.L., de Miranda Cardoso, J.V., Reimer, J., Harrington, J., Rodríguez, J.L.C., Nunez-Iglesias, J., Kuczynski, J., Tritz, K., Thoma, M., Newville, M., Kümmerer, M., Bolingbroke, M., Tartre, M., Pak, M., Smith, N.J., Nowaczyk, N., Shebanov, N., Pavlyk, O., Brodtkorb, P.A., Lee, P., McGibbon, R.T., Feldbauer, R., Lewis, S., Tygier, S., Sievert, S., Vigna, S., Peterson, S., More, S., Pudlik, T., Oshima, T., Pingel, T.J., Robitaille, T.P., Spura, T., Jones, T.R., Cera, T., Leslie, T., Zito, T., Krauss, T., Upadhyay, U., Halchenko, Y.O., Vázquez-Baeza, Y., 2020. SciPy 1.0: fundamental algorithms for scientific computing in Python. Nat Methods 17, 261–272. https://doi.org/10.1038/s41592-019-0686-2

Vogelmann, J.E., Rock, B.N., Moss, D.M., 1993. Red edge spectral measurements from sugar maple leaves. Remote Sensing 14, 1563–1575. https://doi.org/10.1080/01431169308953986

Wahid, A., Close, T.J., 2007. Expression of dehydrins under heat stress and their relationship with water relations of sugarcane leaves. Biol Plant 51, 104–109. https://doi.org/10.1007/s10535-007-0021-0

Walther, G.R., Berger, S., Sykes, M.T., 2005. An ecological 'footprint' of climate change. Proceedings of the Royal Society B: Biological Sciences 272, 1427–1432.

Wang, K., Shao, X., Gong, Y., Zhu, Y., Wang, H., Zhang, X., Yu, D., Yu, F., Qiu, Z., Lu, H., 2013. The metabolism of soluble carbohydrates related to chilling injury in peach fruit

exposed to cold stress. Postharvest Biology and Technology 86, 53–61. https://doi.org/10.1016/j.postharvbio.2013.06.020

Wang, Z., Chlus, A., Geygan, R., Ye, Z., Zheng, T., Singh, A., Couture, J.J., Cavender-Bares, J., Kruger, E.L., Townsend, P.A., 2020. Foliar functional traits from imaging spectroscopy across biomes in eastern North America. New Phytologist 228, 494–511. https://doi.org/10.1111/nph.16711

Weingarten, E., Martin, R., Hughes, F., Vaughn, N., Schafron, E., Asner, G.P., 2021. Early Detection of a Tree Pathogen using Airborne Remote Sensing. Ecological Applications. 21.

Whitham, T.G., Bailey, J.K., Schweitzer, J.A., Shuster, S.M., Bangert, R.K., LeRoy, C.J., Lonsdorf, E.V., Allan, G.J., DiFazio, S.P., Potts, B.M., Fischer, D.G., Gehring, C.A., Lindroth, R.L., Marks, J.C., Hart, S.C., Wimp, G.M., Wooley, S.C., 2006. A framework for community and ecosystem genetics: from genes to ecosystems. Nat Rev Genet 7, 510–523. https://doi.org/10.1038/nrg1877

Xie, L., Ying, Y., Ying, T., 2009. Classification of tomatoes with different genotypes by visible and short-wave near-infrared spectroscopy with least-squares support vector machines and other chemometrics. Journal of Food Engineering 94, 34–39. https://doi.org/10.1016/j.jfoodeng.2009.02.023

Xie, X. j., Zhang, Y. h., Li, R. y., Shen, S. h., Bao, Y. x., 2019. Prediction model of rice crude protein content, amylose content and actual yield under high temperature stress based on hyper-spectral remote sensing. Quality Assurance and Safety of Crops & Foods 11, 517–527. https://doi.org/10.3920/QAS2018.1295

Yan, Z., Guo, Z., Serbin, S.P., Song, G., Zhao, Y., Chen, Y., Wu, S., Wang, J., Wang, X., Li, J., Wang, B., Wu, Y., Su, Y., Wang, H., Rogers, A., Liu, L., Wu, J., 2021. Spectroscopy outperforms leaf trait relationships for predicting photosynthetic capacity across different forest types. New Phytologist 232, 134–147. https://doi.org/10.1111/nph.17579